

# Toward a Better Understanding of Synthesis and Processing of Ceramic/Self-Assembled Monolayer Bilayer Coatings

T.O. SALAMI,<sup>1</sup> Q. YANG,<sup>2</sup> K. CHITRE,<sup>2</sup> S. ZAREMBO,<sup>1</sup> J. CHO,<sup>2,3</sup> and S.R.J. OLIVER<sup>1</sup>

1.—Department of Chemistry, State University of New York at Binghamton, Binghamton, NY 13902-6000. 2.—Department of Mechanical Engineering, State University of New York at Binghamton. 3.—E-mail: jcho@binghamton.edu

Ceramic/self-assembled monolayer (SAM) bilayer coatings can provide adequate protection for silicon devices, or act as a multipurpose coating for other electronic applications, due to synergistic effects by forming a hybrid coating structure. The organic SAM layer acts as a “template” for the growth of the ceramic layer, while the ceramic layer can provide protection from environmental and mechanical impact. Low-temperature solution-based deposition techniques, namely, an in-situ solution method (biomimetic) and a hydrothermal method, have been employed in this study. Specifically, phosphonate-based (diethyl phosphatoethyl triethoxy silane) SAMs were used as a template to generate a zirconia ceramic layer at low temperatures. Other organic templates such as  $-\text{SiCl}_3$ -,  $-\text{OH}$ -,  $-\text{HSO}_3$ -, or  $-\text{CH}_3$ -terminated SAMs were also examined. The reactions to grow the ceramic film were found to be pH sensitive. The ceramic and SAM coatings were characterized by a variety of analytical techniques. A pathway for the formation of the ceramic coating is also discussed.

**Key words:** Ceramic/self-assembled monolayer (SAM), bilayer coatings, zirconia, ceramic layer

## INTRODUCTION

In recent years, research has focused on the development of functional silicon nanodevices in the form of micro-electromechanical systems (MEMS) and nano-electromechanical systems. These systems have prompted the development of several device structures.<sup>1–4</sup> The challenge with these systems, however, includes a stiction problem, the need for a protection coating, and an expensive hermetic packaging requirement that may account for 75–95% of the cost of the systems.<sup>5</sup> Replacing the hermetic packaging with an appropriate, efficient protective coating would considerably lower the cost of the systems, as well as provide a remedy for the stiction problem.

Attempts have been made in the past to create protective coatings for silicon devices. A SAM coating of octadecyltrichlorosilane or perfluorodecyltrichlorosilane was used as a monolayer coating for

polysilicon MEMS by Maboudian and co-workers.<sup>6,7</sup> The properties of the material were not entirely satisfactory because the SAM layers could not withstand harsh conditions. The same authors and Chidsey et al. improved the coating properties using a free radical reaction of a primary alkene (e.g., 1-octadecene  $\text{C}_{16}\text{H}_{33}\text{CH}=\text{CH}_2$ ) with hydrogen-terminated silicon.<sup>8,9</sup> Though a slight improvement in the performance of the coating was observed, the stability of the SAM to elevated temperatures was still a concern.

Ceramic coatings such as  $\text{ZrO}_2$  or  $\text{Y}_2\text{O}_3\text{-ZrO}_2$  can offer a remedy for several problems that organic coatings inherently possess. These films can be deposited by techniques such as sol-gel,<sup>10</sup> plasma spray,<sup>11</sup> or solution deposition.<sup>12</sup> While these coatings give good coverage, high-temperature processing and postannealing steps result in crack formation and film spallations. In this context, ceramic coatings must be strain tolerant to be used as protective layers. Further, the processing temperatures must be low enough in order to allow the surface coatings to

be deposited on microelectronic and MEMS device structures.

The objective of this study is to develop coatings that employ the advantages of organic SAM films while processing hard and stiff inorganic (ceramic) protective coatings. The underlying SAM layer will act as a template for the growth of the ceramic layer. The SAM synthetic strategy is advantageous because the terminal groups can be chemically tailored or functionalized to allow the formation of bonds with the ceramic precursor at very low temperatures. Studies of several such bilayer coatings have been reported in the literature but they all use the sulfonate-terminated SAM with a  $\text{Zr}(\text{SO}_4)_2 \cdot 4\text{H}_2\text{O}$  precursor. A bilayer coating reported by Agarwal et al.<sup>13</sup> used a sulfonate-terminated SAM capped by a ceramic layer ( $\text{Y}_2\text{O}_3$ -doped  $\text{ZrO}_2$ ). Others have reported the same synthesis using a sulfonate-terminated SAM generated by a different synthetic route<sup>14,15</sup> but with similar results.

Earlier work by Mallouk and co-workers<sup>16–18</sup> used a “layer-by-layer” (LbL) synthesis technique. They built organized multilayer molecular assemblies of zirconium 1,10-decanebisphosphonate. This water-insoluble inorganic layered compound contains alternating Zr-O-P inorganic regions connected by a nonpolar alkylene monolayer. The LbL technique is one of the earlier examples of the versatility of multilayer self-assembly architecture chemistry.

We report herein the synthesis and multianalytical characterization of a bilayer coating composed of a phosphonate-terminated SAM and a zirconia top layer. The effects of organic surface (i.e., SAM) on the growth of ceramic films from inorganic precursor solution are highlighted.

## EXPERIMENTAL

In the experiments performed in this study, all of the chemicals were used as received, except toluene (Aldrich, St. Louis, MO), which was distilled. Teflon containers were used unless otherwise specified. Three-inch n-type [100] single crystal silicon wafers (Silicon Quest International, Santa Clara, CA) were cut to about  $1\text{ cm}^2$  by a fracture technique, rinsed in deionized water, and dried under a stream of  $\text{N}_2$  gas. The silicon wafers are then exposed to a freshly prepared Piranha solution [1 part  $\text{H}_2\text{O}_2$  (30% Aldrich) to 3 parts  $\text{H}_2\text{SO}_4$  (Aldrich) by volume] and heated for 1 h in an oil bath maintained at  $70^\circ\text{C}$ . The cleaned wafers are then rinsed with deionized water, followed by drying under a stream of  $\text{N}_2$  gas.

The SAM layer (diethyl phosphatoethyl triethoxy silane) was deposited on the clean wafer by modification of the Sagiv-type siloxane SAM deposition technique.<sup>19</sup> The wafer was exposed to a 5% SAM solution in toluene in a reaction cell under inert atmosphere (Ar), or in a  $\text{N}_2$  glove box, for 24 h. The wafers were rinsed with a fresh portion of toluene, ultrasonically cleaned to remove physically absorbed particles, and dried under a stream of  $\text{N}_2$  gas. The deposited SAM was cured at  $90^\circ\text{C}$  for 1 h.

The ceramic in-situ deposition process was carried out with a freshly prepared 0.01-M solution of  $\text{Zr}(\text{SO}_4)_2 \cdot 4\text{H}_2\text{O}$  (Alfa Aesar, Ward Hill, MA) and 0.4-M HCl (Fisher Scientific, Pittsburgh, PA); another set of samples were prepared in a 0.01-M solution of  $\text{ZrOCl}_2 \cdot 8\text{H}_2\text{O}$  (Alfa Aesar). The SAM-coated and cleaned bare wafers (used as a control) were immersed in the precursor solution for 24 h in an oil bath maintained at  $80^\circ\text{C}$ . The wafers were then removed, rinsed in distilled water, and dried under a stream of  $\text{N}_2$  gas.

In an attempt to carefully examine the characteristics of the precursor solution, it was vacuum filtered to produce precursor powders. Two differently treated solutions were studied: one is the aforementioned in-situ prepared solution, and the other is a hydrothermally treated solution. The hydrothermal process was carried out in an 18-mL capacity Teflon-lined autoclave (constructed in-house). The freshly prepared precursor solution was placed in the autoclave. The autoclave was sealed and placed in a  $125^\circ\text{C}$  oven for 2 to 24 h.

The final coatings and powders were characterized by a variety of techniques. X-ray diffraction (XRD) was used to analyze the crystalline nature of the coatings. The morphology was analyzed by atomic force microscopy (AFM) and low-kV scanning electron microscopy (SEM). The nanoparticle nature of precursor solution and the coatings was analyzed by transmission electron microscopy (TEM). X-ray photoelectron spectroscopy and energy-dispersive x-ray spectroscopy (EDS) were also used to determine the elemental analyses.

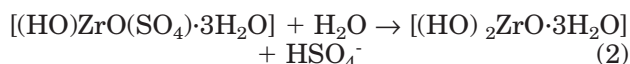
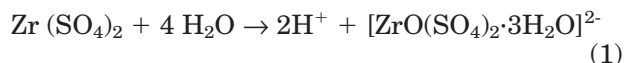
## RESULTS AND DISCUSSION

The chemistry of the SAM precursor and the behavior of the  $\text{Zr}(\text{SO}_4)_2 \cdot 4\text{H}_2\text{O}$  and  $\text{ZrOCl}_2 \cdot 8\text{H}_2\text{O}$  ceramic precursor play a major role in the formation of the bilayer. Several theories have been proposed for the chemistry of these precursors in an aqueous medium, most of which are based on sensitivity to pH. Agarwal et al.<sup>13</sup> proposed the formation of positively charged  $\text{ZrO}_2$  particles based on the  $\text{pK}_a$  of the reaction solution and the isoelectric point of zirconia. Their hypothesis is based on the modification of Derjaguin–Landau–Vervwey–Overbeck theory.<sup>20,21</sup> This theory proposes an increase in the magnitude of attractive forces between particles in solution and an assumption that the particles falling out of solution can be chemically tuned to have opposite charge to a surface/substrate, which allows for deposition on the surface by electrostatic attraction.

The solution behavior for  $\text{ZrOCl}_2 \cdot 8\text{H}_2\text{O}$  (zirconyl chloride octahydrate) can be accounted for by the crystal structure. The dominant zirconium species is in the form of the  $[\text{Zr}_4(\text{OH})_8]^{8+}$  ion,<sup>22</sup> with water molecules grouped around the discrete zirconium ion complexes.<sup>23,24</sup> When the crystal is added to water, it readily dissolves and the zirconium oligomers are removed from the lattice into solution, where they decompose into  $\text{ZrOOH}^+$  units. This cationic hydrolysis

product is a characteristic of zirconium complexes when exposed to a low pH environment.

Similarly, the hydrolysis of the sulfate produces basic anions in solution, as shown in Eqs. 1 and 2.<sup>22</sup> Further hydrolysis yields the same metastable intermediate  $[\text{Zr}_4(\text{OH})_8]^{8+}$  ion from the  $[(\text{HO})_2\text{ZrO} \cdot 3\text{H}_2\text{O}]$  species.



The reactions of the zirconia precursors are pH sensitive because the low pH affords the formation of the metastable ion by hydrolysis. Therefore, it is important to control this parameter to allow the formation of the metastable zirconia. This control would thereby allow the  $[\text{Zr}_4(\text{OH})_8]^{8+}$  to react, bond, or decompose on the underlying SAM layer in situ. Experiments were performed to determine the presence of such particles in solution.

A 0.01-M solution of  $\text{Zr}(\text{SO}_4)_2 \cdot 4\text{H}_2\text{O}$  as well as  $\text{ZrOCl}_2 \cdot 8\text{H}_2\text{O}$  was hydrolyzed, the reaction was quenched prematurely, the solution was filtered, and the resultant powder was then analyzed. A TEM analysis of the resultant  $\text{ZrOCl}_2 \cdot 8\text{H}_2\text{O}$  powder shows the presence of fine particles and agglomerates (Fig. 1a). Its electron diffraction pattern indicated the presence of an amorphous phase for the  $\text{ZrOCl}_2 \cdot 8\text{H}_2\text{O}$  solution (Fig. 1b). Similarly, the powder obtained from the  $\text{Zr}(\text{SO}_4)_2 \cdot 4\text{H}_2\text{O}$  precursor solution also shows an amorphous nature, as can be seen in the XRD pattern (Fig. 2).

In fact, initial raw zirconium sulfate materials contain crystalline particles before hydrolysis reactions. Sintering of both filtered powders at high

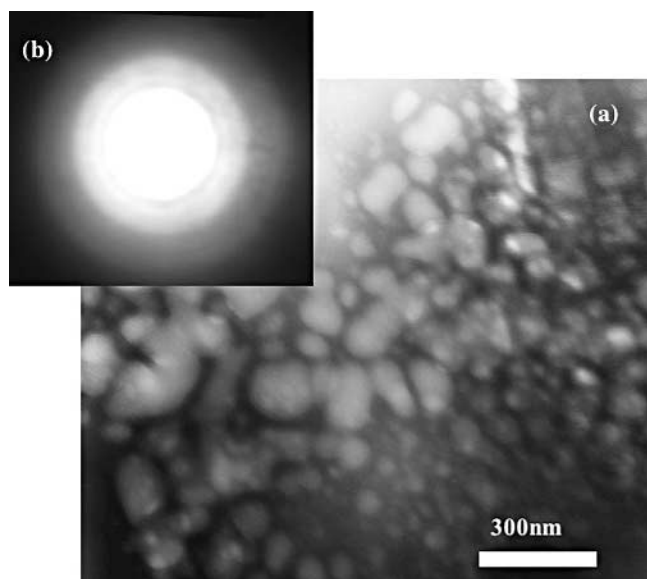


Fig. 1. (a) TEM bright-field image showing fine particles and agglomerates obtained from  $\text{ZrOCl}_2 \cdot 8\text{H}_2\text{O}$  filtered solution. (b) Corresponding electron diffraction pattern confirming the presence of an amorphous phase for  $\text{ZrOCl}_2 \cdot 8\text{H}_2\text{O}$  solution.

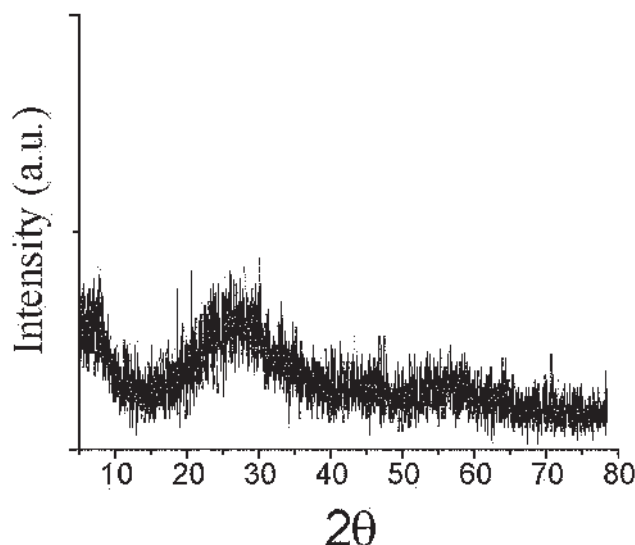


Fig. 2. XRD pattern of the powder for  $\text{Zn}(\text{SO}_4)_2 \cdot 4\text{H}_2\text{O}$ -filtered solution showing the amorphous nature of the precursor.

temperatures ( $>950^\circ\text{C}$ ) yielded a mixed  $\text{ZrO}_2$  phase (tetragonal and monoclinic). In addition, the amorphous nature of the analyzed powders suggests some form of amorphous  $\text{Zr}(\text{OH})_4$  phase. This observation further proves that the metastable phase of zirconia ion usually decomposes in solution. It is therefore important to find a condition in which the metastable zirconia ions bond directly to a receptive SAM layer in situ.

In light of these results, hydrothermal treatments of the  $\text{ZrOCl}_2 \cdot 8\text{H}_2\text{O}$  precursor were performed at high pH. The solutions were adjusted to a pH of 10 using NaOH pellets. The mixture was hydrothermally treated at  $125^\circ\text{C}$  for 24 h under autogenous pressure and the product was vacuum filtered. The TEM analysis reveals submicron sized particles (Fig. 3a) and crystalline phases, as shown in the electron diffraction pattern (Fig. 3b). The presence of tetragonal ("t") and monoclinic ("m") zirconia phase was also confirmed by powder XRD (Fig. 3c). The hydrothermal preparation of this bulk material under autogenous pressure promoted a crystalline  $\text{ZrO}_2$  phase at relatively low temperatures in contrast to the resultant amorphous phases from the in-situ solution treatment discussed earlier.

The SAM terminal functionality thus needs to be tuned chemically to allow (1) formation of a bond between the SAM and the ceramic layer or (2) for the SAM to act as a template for the growth of the ceramic layer. This goal, however, remains a challenge. If the chemistry is better understood, then a rational design of bilayer coatings with custom properties becomes straightforward. Various SAM functionalities such as  $-\text{SiCl}_3$ ,  $-\text{OH}$ ,  $-\text{HSO}_3$ , or  $-\text{CH}_3$  were used in our preliminary study.<sup>25</sup> Some of these are available commercially, while the  $-\text{HSO}_3$  and  $-\text{OH}$  termini have been synthesized. The  $-\text{HSO}_3$  terminus was synthesized from an alkene-terminated SAM exposed to  $\text{SO}_3$ , while the  $-\text{OH}$ -terminated SAM



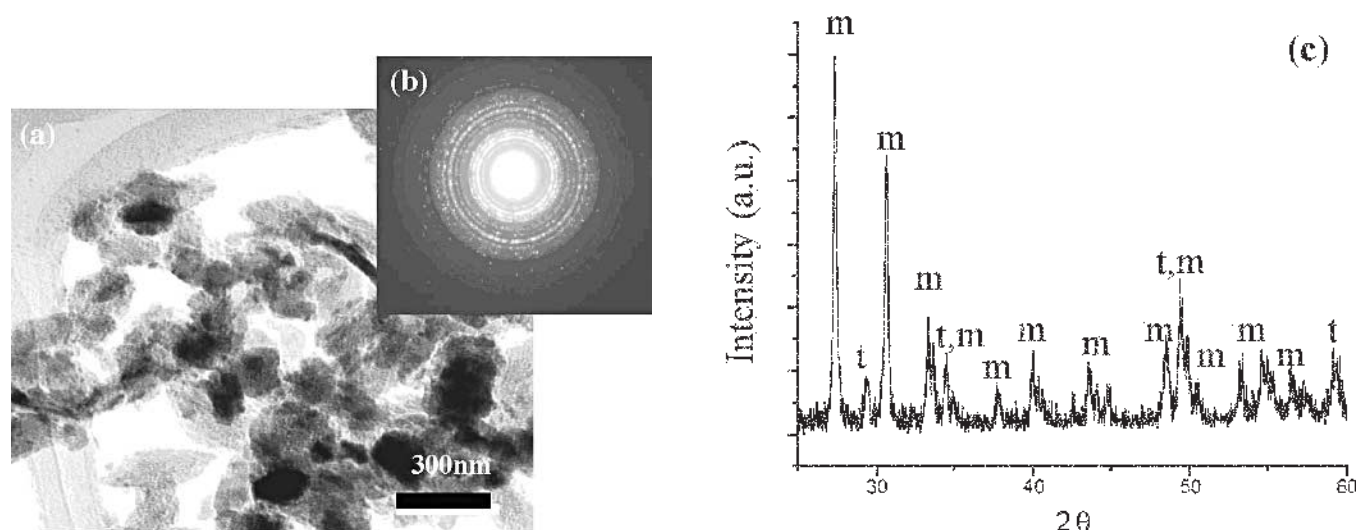


Fig. 3. (a) TEM bright-field image of hydrothermally synthesized crystalline zirconia particles. (b) Corresponding electron diffraction pattern indicative of the crystalline nature of the particles. (c) XRD pattern showing the t- and m-zirconia phases.

was synthesized from an acetate-terminated SAM, reduced by  $\text{LiAlH}_4$  followed by acid hydrolysis. The  $-\text{POR}_3\text{H}$ -terminated SAM was acquired from a commercial vendor.

It is also shown that surface functionality and uniformity of SAM play an important role in the growth of ceramic films. The surface conditions were investigated for substrate coverage of SAMs. For example, the  $-\text{Cl}$ -terminated SAM had low coverage and exhibits formation of islands when compared to the phosphonate-terminated SAM (PO-SAM) (Fig. 4). The solution deposition technique for other SAMs such as  $-\text{OH}$ , and  $-\text{CH}_3$  termini resulted in very low coverage. This is partly due to the hydrophobic nature of the SAM terminus that does not encourage the interaction of the precursor with the SAM layer.

It should be noted, however, that a hydrophilic surface alone does not influence ceramic growth.<sup>26</sup> The  $-\text{HSO}_3$  functionality is a viable choice and has been extensively studied and reported elsewhere.<sup>13–15</sup> Our choice of a phosphonate-terminated SAM for the bilayer coating is influenced by the rich chem-

istry of zirconium phosphonates that is affordable. Our system, however, involves the formation of monolayers with either zirconium sulfate or zirconyl chloride precursor. Experiments carried out with zirconium sulfate exhibited a better surface coverage on Si- and SAM-coated Si under acidic conditions. Zirconyl chloride displayed a better coverage under basic conditions.

Contact angle measurement was used to monitor overall quality and surface modification of the SAM coating. The Piranha-cleaned wafer had an average water contact angle of approximately  $5^\circ$ , indicating a very hydrophilic surface (Table I). On deposition of the PO-SAM (from diethyl phosphatoethyl triethoxy silane), the average contact angle became  $90^\circ$  (Table I), typical of the hydrophobic nature for this type of SAM.

Ceramic deposition from zirconium sulfate precursors by the solution technique on the PO-SAM-deposited silicon wafer led to localized ceramic coverage on the silicon surface. The chemistry of the SAM terminus requires the  $(\text{RO})_2\text{PO}-$  bond to be converted to  $(\text{HO})_2\text{PO}-$  bonds. This conversion can be performed

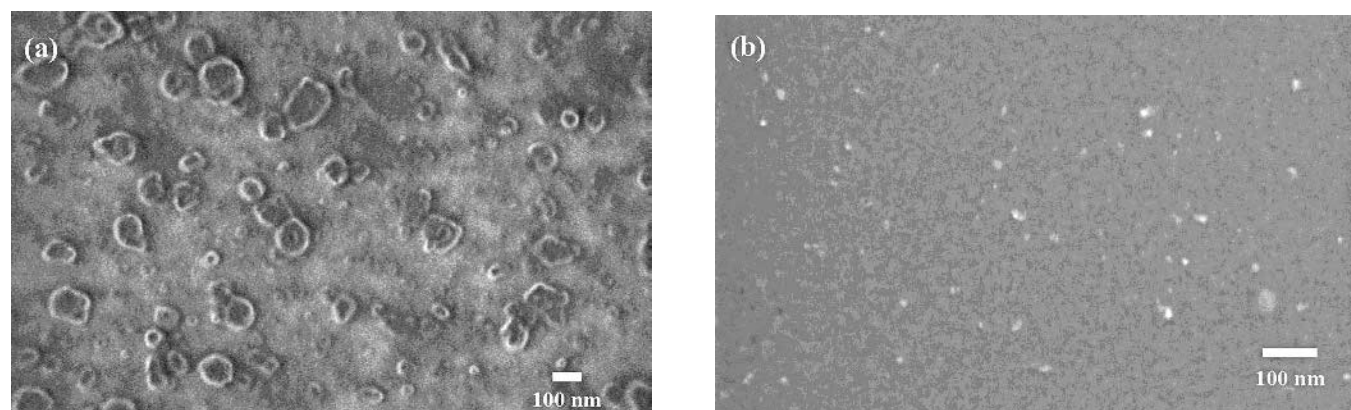


Fig. 4. SEM micrographs of the SAM coatings: (a)  $-\text{Cl}$ -terminated SAM shows islands with rough and incomplete coverage; and (b) smooth coverage of the  $-\text{PO}$ -terminated SAM.

**Table I. Water Contact Angle Measurement for Various Substrates**

Description	Water Contact Angle (°)
Bare wafer	45°
Piranha-cleaned bare wafer	5°
–POHR <sub>2</sub> -deposited SAM	90°
–POHR <sub>2</sub> after HCl acid hydrolysis	30°
After ceramic deposition	97°

by HCl acid hydrolysis<sup>27</sup> or refluxing in bromotrimethylsilane (3 equiv) in dichloromethane.<sup>28,29</sup> The SAM-covered silicon wafers were treated in 1-M HCl for a period of 30, 60, 90, or 120 min in an oil bath set at 70°C before ceramic deposition. The contact angle measured after the acid treatment was approximately 30° (Table I). The acid-treated sample does not show a significant change in the contact angle for longer immersion times, thereby reducing only slightly after 30 min.<sup>28</sup> This leads to the assumption that the surface is modified based on the variation in contact angle. Further reactions can also be carried out by variation of the concentration and reflux time. Higher HCl concentration and more harsh conditions may, however, destroy the SAM layer. Interestingly, the contact angle of the ceramic-coated film was very hydrophobic (97°), which shows a great potential for antistiction coating applications.

The films prepared using  $\text{Zr}(\text{SO}_4)_2 \cdot 4\text{H}_2\text{O}$  were characterized to determine their properties. The AFM image in Fig. 5 shows a particulate film structure with a wide range of spherical particles. In some regions, interparticle neck formation can be seen, and most of the large particles seem to float in a top layer, indicating a process of settling from the solution phase. The TEM also confirmed the presence of a continuous film above the silicon wafer (Fig. 6a). The TEM-EDS for the corresponding areas shows the presence of Zr (Fig. 6b and c). The film structure seems to be amorphous, as can be seen in Fig. 7, which is in agreement with the quenching experiments. Post-thermal treatments above 1,000°C transformed the films to tetragonal and monoclinic zirconia phases. In addition, some oxide peaks from the Si substrate were found in the

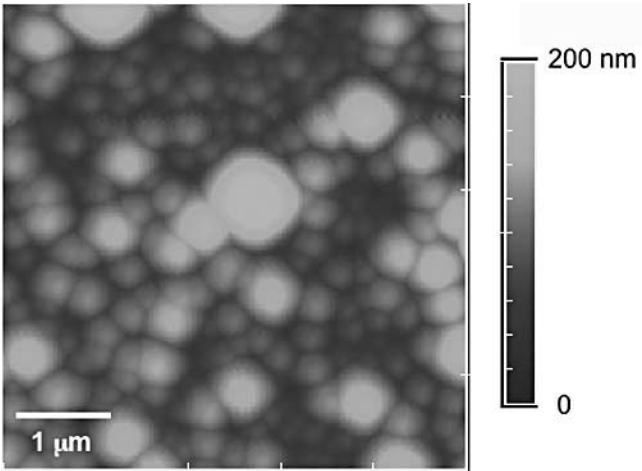


Fig. 5. AFM image of zirconia ceramic coating on PO-SAM displaying a wide range of particle size and some densely packed areas (xy scan:  $5 \times 5 \mu\text{m}^2$ ; z scan: 200 nm).

XRD patterns (appearing below  $2\theta = 30^\circ$ ) even for the as-deposited film.

It should be noted that no continuous film was observed for the ceramic growth on bare Si and untreated SAM. This indicates the template effect due to the SAM layer. The proposed mode of formation of  $\text{ZrO}_2$  on the SAM layer is presented in Fig. 8. This is based on an acid hydrolysis of the alkyl phosphonate to the corresponding phosphonic acid derivative. It mimics the biological growth of inorganic (ceramic) films on the surface of organic substances (biomimetic growth). Further study is needed to better understand this growth model, since the film produced thus far is rather amorphous in nature. A retardation of crystallization resulting in amorphous structure of the film can be related to C and Si contamination during growth. The mechanical properties and the numerical modeling of the system, discussed here, have been reported earlier.<sup>30</sup>

### CONCLUSIONS

The work presented in the above study shows the formation of a bilayer by bonding a zirconia precursor to a PO-SAM using a solution precursor technique. The SAM layer was used as a template to produce the ceramic layer. The formation of a metastable zirconia ion in solution is in situ and pH dependent. In

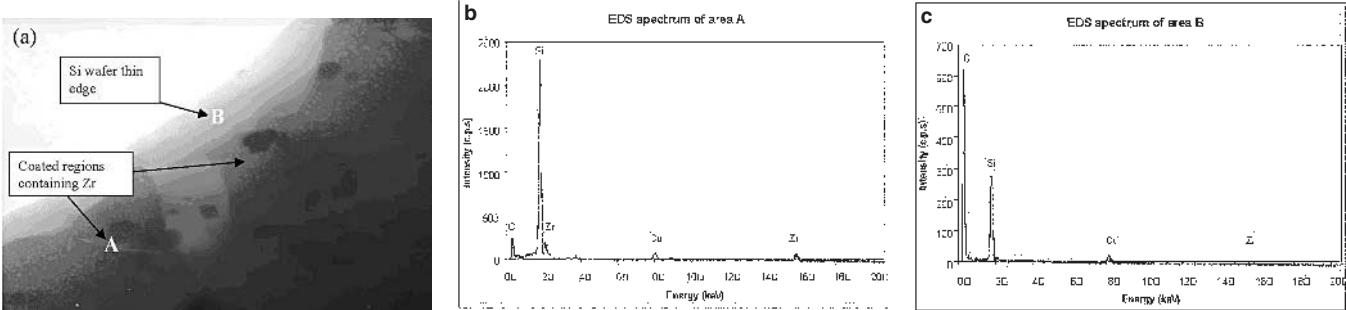


Fig. 6. (a) Plan-view TEM bright-field image of cleaved-ceramic coating, which was deposited in solution in situ at 80°C (on Si substrate); (b) EDS of area A showing Zr peak; and (c) EDS of area B showing Si and strong C peaks.

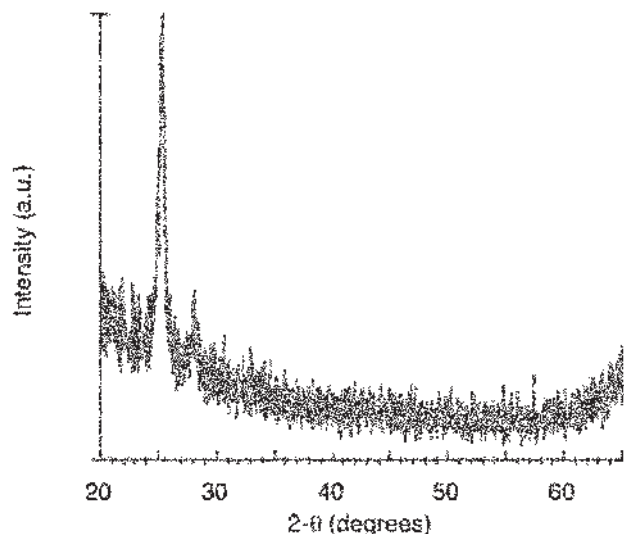


Fig. 7. XRD characterization for the in-situ solution-prepared coating at 80°C. Note that the two low-angle peaks below  $2\theta = 30^\circ$  are from the substrate.

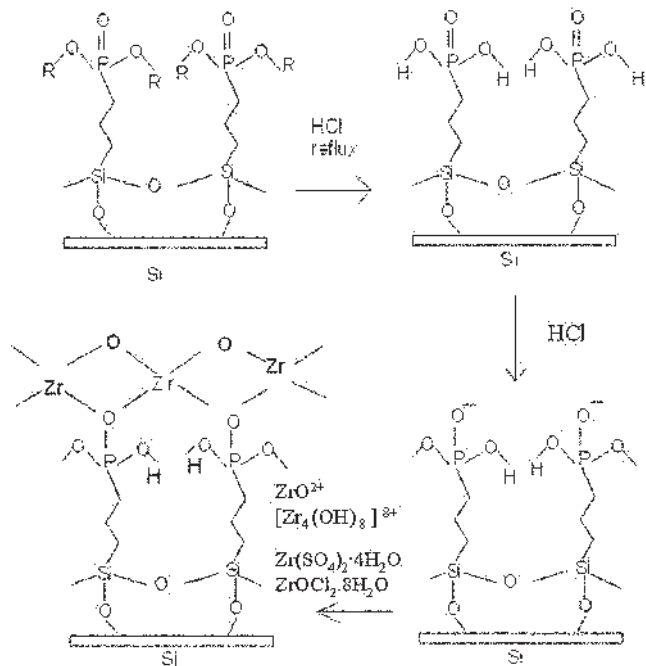


Fig. 8. Proposed reaction pathways for the formation of the  $\text{ZrO}_2$  layer grown on a phosphonate ( $-\text{PO}$ ) terminated SAM.

addition, the SAM terminus must be sufficiently reactive to form a bond with the metastable zirconia ion. An analysis of the resultant powder from a quenched reaction established that the reaction of the metastable ion occurs in situ, but it did not show crystalline structure until heat treated at high temperatures. Tetragonal and monoclinic zirconia phases were generated from hydrothermal treatment of bulk material in a basic medium at 125°C. The in-situ prepared ceramic films were very hydrophobic. A better understanding of the mechanism concerning formation of these coatings would be a significant step toward the synthesis of bilayer coatings with desired properties.

## ACKNOWLEDGEMENTS

This work was funded by Infotonics Technology Center Inc. (U.S. DOE Grant No. DE-FG02-02ER63410.A000) and partially supported by the Integrated Electronic Engineering Center (IEEC) at SUNY-Binghamton. The authors thank X. Wang, C. McConville, and Y. Liu, Alfred University, and M. Coy, JEOL, for helping with some of the characterization techniques.

## REFERENCES

- Edward S. Kolesar, William E. Odom, Joseph A. Jayachandran, Matthew D. Ruff, Simon Y. Ko, Jeffery T. Howard, Peter B. Allen, Josh M. Wilken, Noah C. Boydston, and Jorge E. Bosch, *Thin Solid Films* 447–448, 481 (2004).
- Heather H. DiBiao, Brian A. English, and Mark G. Allen, *Sensors and Actuators A: Physical* 111, 260 (2004).
- A.Q. Liu, X.M. Zhang, J. Li, and C. Lu, *Sensors and Actuators A: Physical*, 108, 49 (2003).
- C. Lee, E.-H. Yang, N.V. Myung, and T. George, *Nano Lett. (Comm.)* 3, 1339 (2003).
- N. Maluf, *An Introduction to Microelectromechanical Systems* (Inc., Norwood, MA: Artech House, 2000).
- M.R. Houston, R. Maboudian, and R.T. Howe, *7th Solid-State Sensor and Actuator Workshop*, Hilton Head Island, SC, June 2–6, 1996, pp. 42–47.
- U. Srinivasan, M.R. Houston, R.T. Howe, and R. Maboudian, Alkyltrichlorosilane-based self-assembled monolayer films for stiction reduction, *IEEE/ASME J. Micro-electromechanical Systems*, 7, 252 (1998).
- M.R. Linford, P. Fenter, P.M. Eisenberger, and C.E.D. Chidsey, *J. Am. Chem. Soc.* 117, 3145 (1995).
- M.M. Sung, G.J. Kluth, O.W. Yauw, and R. Maboudian, *Langmuir* 13, 6164 (1997).
- X. Changrong, C. Huaqiang, W. Hong, Y. Pinghua, M. Guangyao, and P. Dingkun, *J. Membrane Sci.* 162, 181 (1999).
- A. Kulkarni, A. Vaidya, A. Goland, S. Sampath, and H. Herman, *Mater. Sci. Eng. A*, 359, 100 (2003).
- C. Xia, S. Zha, W. Yang, R. Peng, and D. Peng, *Solid State Ionics* 133, 287 (2000).
- M. Agarwal, M.R. De Guire, and A.H. Heuer, *J. Am. Ceram. Soc.* 80, 2967 (1997).
- J. Wang, S. Yang, X. Liu, S. Ren, F. Guan, and M. Chen, *Appl. Surface Sci.* 221, 272 (2004).
- V.V. Roddatis, D.S. Su, E. Beckmann, F.C. Jentoft, U. Braun, J. Krohnert, and R. Schlogl, *Surface Coatings Technol.* 151–152, 63 (2002).
- H. Lee, L.J. Kepley, H.-G. Hong, and T.E. Mallouk, *J. Am. Chem. Soc.* 110, 618 (1988).
- H.-G. Hong, D.D. Sackett, and T.E. Mallouk, *Chem. Mater.* 3, 521 (1991).
- J. Kepley, D.D. Sackett, C.M. Bell, and T.E. Mallouk, *Thin Solid Films* 208, 132 (1992).
- J. Sagiv, *J. Am. Chem. Soc.* 102, 92 (1980).
- B.V. Derjaguin and L.D. Landau, *Acta Physicochim. USSR* 14, 733 (1941).
- E.J.W. Verwey and J.T.G. Overbeek, *Theory of Stability of Lyophobic Colloids* (Amsterdam, The Netherlands: Elsevier, 1948).
- W.B. Blumenthal, *The Chemical Behavior of Zirconium* (New York: D. van Nostrand Co., 1958), chs. 3, 4, and 6.
- A. Clearfield and P.A. Vaughan, *Acta Cryst.* 9, 555 (1956).
- B.T. Meyer, *Naturwiss* 118, 34 (1930).
- Q. Yang, T. Salami, K. Chitre, S. Oliver, and J. Cho, unpublished work (State University of New York at Binghamton, 2004).
- K. Chitre, Q. Yang, T.O. Salami, S.R. Oliver, and J. Cho, *J. Electron. Mater.* 34, 528, 2005.
- A. Aliev, D. Li Ou, B. Ormsby, and A.C. Sullivan, *J. Mater. Chem.* 10, 2758 (2000).

28. R. Frantz, M. Granier, J.-O. Durand, and G.F. Lanneau, *Tetrahedron Lett.* **43**, 9115 (2002).
29. C.M. Timperley, M. Bird, I. Holden, and R.M. Black *J. Chem. Soc., Perkin Trans. 1*, 26 (2001).
30. Q. Yang, T.O. Salami, K. Chitre, S.R. Oliver, and J. Cho, *Mechanical Properties of Nanostructured Materials and Nanocomposites*, MRS Proc. (Warrendale, PA: Materials Research Society, 2004), vol. 791, pp. 105–10.